Doping dependence of the ultrafast electronic dynamics of $Y_{1-x}Pr_xBa_2Cu_3O_{7-\delta}$ thin-film superconductors from femtosecond optical spectroscopy

C. W. Luo,[1] H. P. Lo,[1,2] C. H. Su,[1] I. H. Wu,[1] Y.-J. Chen,[1] K. H. Wu,[1] J.-Y. Lin,[3] T. M. Uen,[1] J. Y. Juang,[1] and T. Kobayashi[1,4]

[1]*Department of Electrophysics, National Chiao Tung University, Hsinchu, Taiwan, Republic of China*

[2]*Department of Physics, National Tsing Hua University, Hsinchu, Taiwan, Republic of China*

[3]*Institute of Physics, National Chiao Tung University, Hsinchu, Taiwan, Republic of China*

[4]*Department of Applied Physics and Chemistry, Institute for Laser Science, The University of Electro-Communications, Tokyo, Japan*

(Received 7 May 2010; revised manuscript received 30 July 2010; published 17 September 2010)

Time-domain spectroscopy, which probes the dynamics of the electronic states near Fermi surface that are associated with superconductivity, has proven to be a powerful method for providing insights into the fundamental nature of both pseudogap and superconducting gap. This study shows that the unique *T*-*x* phase diagram with the time-evolving ultrafast dynamics of $Y_{1-x}Pr_xBa_2Cu_3O_{7-\delta}$ can be used to identify clearly the Nernst, pseudogap, and superconducting regions. All of the orders appear together at a specific delay time, such as 1.2–3 ps, after pumping by an ultrashort pulse. These discoveries suggest that the Nernst effect, the pseudogap and even superconductivity may have the same physical origin.

DOI: 10.1103/PhysRevB.82.104512 PACS number(s): 74.25.Gz, 74.78.−w, 74.81.Bd, 78.47.−p

I. INTRODUCTION

Elucidation of phase diagrams has been one of the most demanding challenges of high-T_c superconductivity research. Recently, a large Nernst signal was observed in many hole-doped cuprates at temperatures well above the zero-field T_c.[1–4] Moreover, the onset appearance of a substantial Nernst signal appearing at temperatures that are significantly above T_c in underdoped cuprate superconductors was interpreted for the existence of superconducting fluctuations and vortex-like excitations in the pseudogap phase.[1,4] However, the origin of the Nernst effect and the relationship between the Nernst effect and the pseudogap (or superconductivity) remains to be elucidated.

To understand the underlying physics of the giant Nernst response, many theoretical approaches have been suggested. Vortex motion[5] and superconducting fluctuation[6] are considered to be the two most probable mechanisms. While the former is specific to cuprate superconductors, the latter is believed to be more general and can also be applied to other, more conventional superconductors. Furthermore, the Nernst effect has been identified, by thermoelectric experiments,[4] as a sensitive indicator of superconducting fluctuations. Since the Nernst region extends well above T_c and overlaps with the pseudogap region in the underdoped phase diagram, the anomalous Nernst effect may be related to the pseudogap phenomenon.[6] The general consensus on the results of all time-resolved spectroscopy experiments is that the amplitude and picosecond-scale relaxation time of the transient reflectivity change ($\Delta R/R$) are directly associated with the opening of the superconducting gap below T_c (Refs. 7–10) and related to the appearing of the pseudogap above T_c.[7,10–12] Experiments that are performed in this study conclusively reveal the photoinduced excitations in the Nernst region as well as their evolutions with the delay time. Above T_c, a drastic change in the amplitude of $\Delta R/R$ was clearly observed. The temperature (T_N) that corresponds to the peak in the temperature-dependent $\Delta R/R$ is closely related to the onset temperature of the anomalous Nernst signal. The dynamics of the photoinduced quasiparticles (QPs) in the Nernst, pseudogap and superconducting regions, are distinctive and yield a unique time-evolving ultrafast dynamics phase diagram.

II. EXPERIMENTS

Well characterized (001) $Y_{1-x}Pr_xBa_2Cu_3O_{7-\delta}$ thin films with x=0, 0.1, 0.2, and 0.4 used in this study were prepared on (100) $LaAlO_3$ substrates by pulsed laser deposition. The lattice mismatch between the substrates and a-axis of $Y_{1-x}Pr_xBa_2Cu_3O_{7-\delta}$ thin films is ~0.9%. The thickness of all films is 300 nm, which were measured by α step. In addition, the orientation of all films was characterized to be c-axis epitaxial by x-ray diffraction patterns. Figure 1 shows that

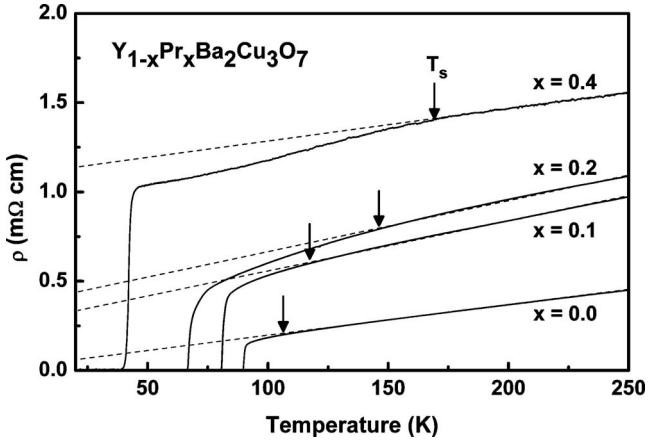

FIG. 1. Electrical resistivity as a function of temperature for $Y_{1-x}Pr_xBa_2Cu_3O_{7-\delta}$ films with x=0, 0.1, 0.2, and 0.4. Arrows indicate temperature T_s, which is defined as the high temperature at which the curve of resistivity against temperature deviates from linearity (dashed lines).

the T_c of various Pr-doped YBCO thin films with $x=0$, 0.1, 0.2, and 0.4 were 89.6 K, 80.5 K, 66.5 K, and 39.4 K, respectively. The spin-gap (or pseudogap) temperature (T_s) was clearly determined by the deviation from the linearity of resistivity as a function of temperature.[13] Samples were mounted on the cold finger of a Janis flow through cryostat and the temperature was measured using a thermometer that was installed close to samples. Femtosecond time-resolved spectroscopy was carried out using the standard pump-probe scheme.[12] Pump-probe measurements were performed using a mirror-dispersion-controlled mode-locked Ti:sapphire laser, which produces a 75 MHz train of 30 fs pulses with a central wavelength of 800 nm. The laser beam was divided into an intensive pump beam and a weak probe beam with cross polarized by a beam splitter. The fluence of the pump beam was kept at 4.35 $\mu J/cm^2$ to cause ~11 K rise near T_c inside the illuminated area while that of the probe beam was kept at 0.26 $\mu J/cm^2$. The probe pulses were delayed with respect to the pump pulses by a computer-controlled delay stage. The penetration depth in 800 nm is around 100 nm.[14] The small reflecting signals were detected by a lock-in amplifier that was referenced at the chopping frequency of 97 kHz.

III. RESULTS AND DISCUSSION

Figures 2(a)–2(d) plot the respective $\Delta R/R$ of the $Y_{1-x}Pr_xBa_2Cu_3O_{7-\delta}$ thin films with $x=0$, 0.1, 0.2, and 0.4, obtained at various temperatures. In the normal state, the process of a large number of QPs which are excited by a pump pulse relax to states close to the Fermi surface (E_F) by either electron-electron or electron-phonon scattering usually occurs on a subpicosecond time scale.[7,11,14] A gap near E_F, however, leads to carrier accumulation in the QP states above the gap at $T<T_c$, which in turn gives rise to a $\Delta R/R$, which was detected by a probe pulse as a function of the delay time (t) between a pump pulse and a probe pulse. The amplitude and characteristic relaxation time of the measured $\Delta R/R$ thus provide important information about the magnitude of the gap and the number of accumulated QPs (N_{QP}): $|\Delta R/R| \propto N_{QP}$.[8,9,11,12] The relaxation time for various Pr-doped samples was obtained by fitting with a single exponential decay function. For $Y_{0.9}Pr_{0.1}Ba_2Cu_3O_{7-\delta}$ and $Y_{0.8}Pr_{0.2}Ba_2Cu_3O_{7-\delta}$ thin films, the relaxation time was obtained from the negative signal above T_c and positive signal below T_c. For $Y_{0.6}Pr_{0.4}Ba_2Cu_3O_{7-\delta}$ thin films, the relaxation time was obtained from the positive signal above T_c and negative signal below T_c. Figure 4 quantitatively represents the aforementioned characteristics by plotting $\Delta R/R$ as a function of temperature. In the case of $YBa_2Cu_3O_{7-\delta}$, the amplitude of the positive component in $\Delta R/R$ rises dramatically near T_c, suggesting the opening of the superconducting gap.[7–12] Earlier works have overlooked the significant change in the rather small and negative component that occurs well above T_c. For comparison, the temperature T_N [marked by an arrow in Fig. 4(a)] that corresponds to the peak of the negative component in the temperature-dependent $\Delta R/R$ coincides surprisingly well with the onset temperature of the anomalous Nernst signal that was observed by Wang *et al.*[1] Similar characteristics of the temperature-dependent $\Delta R/R$ are also observed in Pr-doped YBCO with $x=0.1$ and 0.2, as shown in Figs. 4(b) and 4(c), respectively. As the temperature declines, the negative component gradually rises, reaching its maximum at T_N. This striking change in the negative component may be due to the appearance of the Fehrenbacher-Rice band.[15] When the temperature passes below T_N, the amplitude of the negative component of $\Delta R/R$ decreases, until it becomes vanishingly small at the superconducting temperature T_c, at which the positive component of $\Delta R/R$ starts to emerge while the relaxation time of QPs diverges[7] near T_c. Surprisingly, T_N shifts to lower temperatures as Pr doping increases, and hole concentration therefore declines.

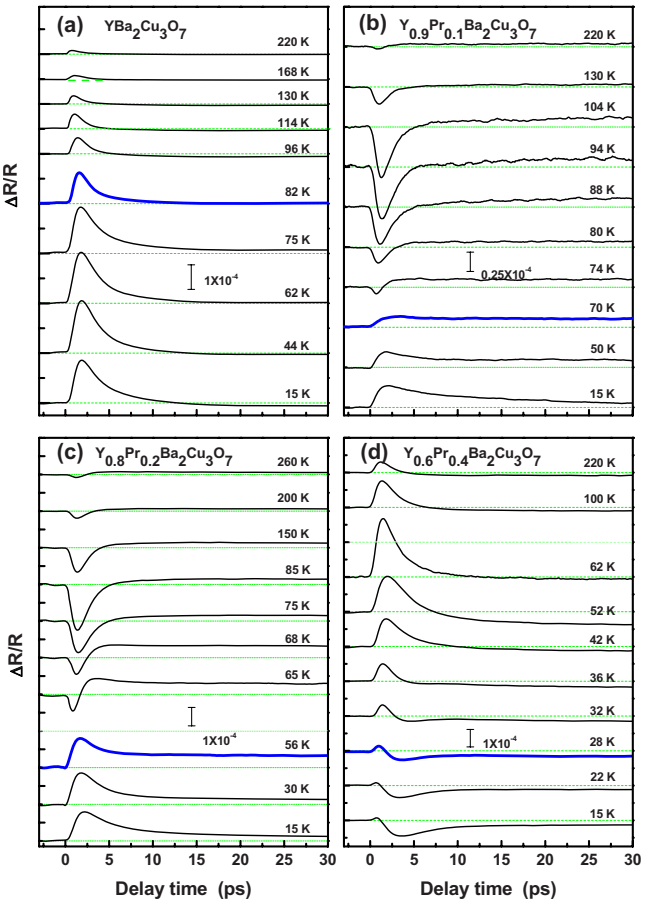

FIG. 2. (Color online) Temperature dependence of $\Delta R/R$ (a) measured in a (001) $YBa_2Cu_3O_{7-\delta}$ film with $T_c=89.6$ K; (b) measured in a (001) $Y_{0.9}Pr_{0.1}Ba_2Cu_3O_{7-\delta}$ film with $T_c=80.5$ K; (c) measured in a (001) $Y_{0.8}Pr_{0.2}Ba_2Cu_3O_{7-\delta}$ film with $T_c=66.5$ K; and (d) measured in a (001) $Y_{0.6}Pr_{0.4}Ba_2Cu_3O_{7-\delta}$ film with $T_c=39.4$ K. Bars indicate vertical scale. Thick lines indicate the temperature of around T_c-11 K (11 K is due to the laser heating). The temperatures of sample holder are marked in this figure.

Similar phenomena were also observed in the most underdoped case ($x=0.4$) in this study, although the sign of the temperature-dependent $\Delta R/R$ is reversed in this case, as shown in Fig. 2(d). At this doping level, the doping-induced shifting in Fermi energy E_F causes the component that is associated with superconductivity to become negative and the component that appears primarily at temperatures above

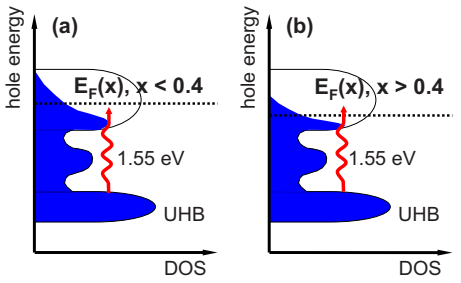

FIG. 3. (Color online) The schematic energy band structure of $Y_{1-x}Pr_xBa_2Cu_3O_{7-\delta}$. DOS: density of state. UHB: upper Hubbard band. E_F: Fermi energy.

T_c to be positive. In 1991, Kazeroonian *et al.*[16] observed a monotonic decrease in E_F as Pr doping increased. They found that the E_F lies 2.0 eV above the upper Hubbard band (UHB) for $x=0.12\pm0.02$. Afterward, the present authors' earlier results show that the E_F decrease to 1.55 eV above UHB at $x=0.4$ by the sign change in $\Delta R/R$ at room temperature.[17] Therefore, the down shifting of E_F with increasing Pr doping as shown in Figs. 3(a) and 3(b) causes the probing energy (1.55 eV) to eventually get close to the difference between E_F and the UHB for the case of $x=0.4$, and then the sign of $\Delta R/R$ to become negative when the superconducting gap opens.[18] One of the explanations for this is, when the sample at superconducting state is illuminated by ultrashort pulses, the density of states (DOS) lying near the Fermi level, with the distribution of Van Hove singularity,[19]

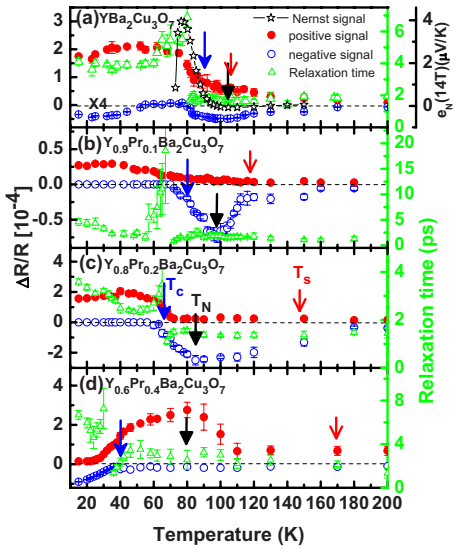

FIG. 4. (Color online) Amplitude (determined from maximum and minimum values of $\Delta R/R$ curves in Fig. 2) and relaxation time of $\Delta R/R$ vs temperature in a (001) (a) $YBa_2Cu_3O_{7-\delta}$ film; (b) $Y_{0.9}Pr_{0.1}Ba_2Cu_3O_{7-\delta}$ film; (c) $Y_{0.8}Pr_{0.2}Ba_2Cu_3O_{7-\delta}$ film; and (d) $Y_{0.6}Pr_{0.4}Ba_2Cu_3O_{7-\delta}$ film. The black arrows show T_N at which the negative (positive) component is minimum (maximum). The red and blue arrows show T_s and T_c, respectively, which were obtained from Fig. 1. The Nernst signal in (a) was taken from Fig. 4 in Ref. 1. The temperatures shown in this figure is the temperature of sample holder. The temperature inside the illuminated spot should consider the extra temperature rise due to laser heating effect, e.g., 90 K (near T_c) +11 K.

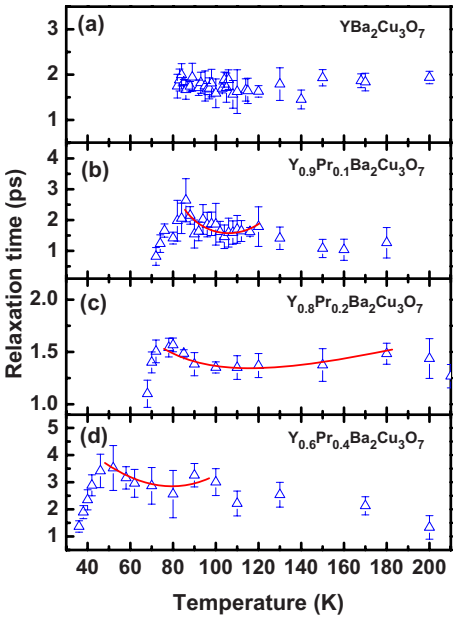

FIG. 5. (Color online) The temperature-dependent relaxation time on an enlarged scale of Fig. 4. The solid line are a guide to the eyes. The temperatures shown in this figure is the temperature of sample holder. The temperature inside the illuminated spot should consider the extra temperature rise due to laser heating effect, e.g., 90 K (near T_c) +11 K.

will change drastically and then modify the Fermi smearing. This abrupt change can be monitored only when the probe energy is close to the energy difference between E_F and UHB and leads to the sign reversal of $\Delta R/R$. As mentioned above, the T_N indicated by the arrows in Fig. 4 gradually decreases as Pr content in YBCO increases, which result is consistent with the Nernst effect that was measured in almost identical $Y_{1-x}Pr_xBa_2Cu_3O_7$ films by Li *et al.*,[2] who found a rapid rise of the Nernst signal at a particular temperature that depends on the Pr concentration [the crosses in Figs. 6(b) and 6(c)]. Thus, the peak in temperature-dependent $\Delta R/R$ above T_c may be caused by the Nernst effect. It means that more photoinduced QPs near Fermi surface are generated and detected by laser pulses[11] due to the preform pairs in the vicinity of Fermi surface around T_N. In the superconducting fluctuation region between T_c and T_N, however, parts of the preform pairs have further formed the cooper pairs to lead the shrink of $\Delta R/R$ as shown in Fig. 2.

Figure 6 presents snapshots of the contours of the amplitude of $\Delta R/R$ signal on the T-x plane at different time after the films were pumped by the femtosecond pulses. The contours, to some extent, effectively illustrate the time evolution of various orders and excitations over the entire T-x phase diagram. At very short delay time within $t=0.5$ ps [Fig. 6(a)], the faint features in the entire phase diagram show a weak and positive $\Delta R/R$ signal in the low-temperature region while a weak and negative $\Delta R/R$ signal is observed around the high-temperature region. Similarly, no significant feature is observed at delays of longer than 10 ps, as shown in Fig. 6(d). Nevertheless, at the delay time of $t=1.2$ and 3 ps, rich features that signal the emergence and dimming of the positive and negative components of $\Delta R/R$ appear in

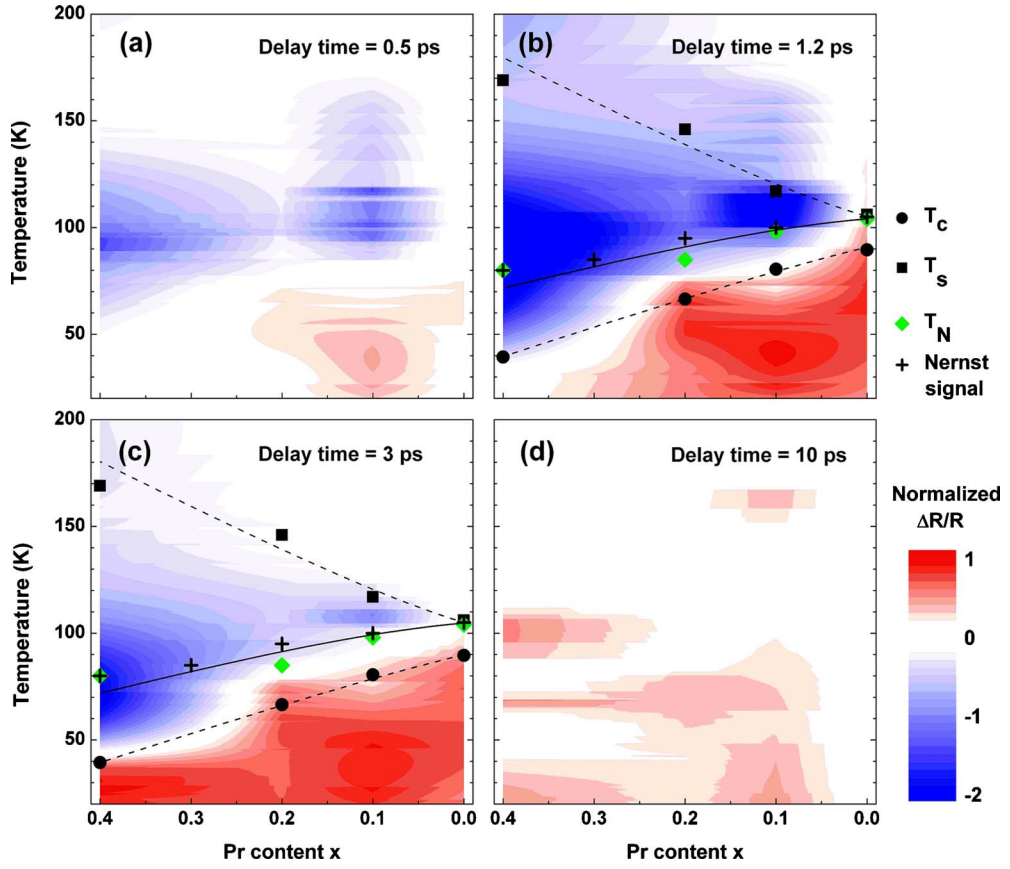

FIG. 6. (Color online) Normalized $\Delta R/R$ as a function of temperature (T) and Pr content (x) at various delay time between pump and probe pulses. T_c (solid circles) is the superconducting transition temperature. T_s (solid squares) is the temperature at which the curve of resistivity vs T in Fig. 1 deviates from linearity. T_N (solid diamonds) is the temperature indicated by the arrows in Fig. 4. The crosses were taken from the onset temperature in the Nernst signal reported by Li *et al.* (Ref. 2). All of the dashed, dotted, and solid lines are guides for the eyes, emphasizing the behavior of T_c, T_s, and T_N. Note: the signs of the positive component and the negative component in $\Delta R/R$ for $x=0.4$ have been reversed here to ensure consistency of contour plotting with $x=0$, 0.1, and 0.3.

different parts of the T-x phase diagram. For instance, all of the positive $\Delta R/R$ (negative $\Delta R/R$ for $x=0.4$ in Fig. 4) that are related to the superconductivity are spread inside the dome of T_c, which is marked by the dashed lines in Figs. 6(b) and 6(c). However, the negative $\Delta R/R$ signal (and positive $\Delta R/R$ for $x=0.4$) appears only at temperatures above T_c. In particular, the areas with larger negative $\Delta R/R$ signals (dark blue) emerge around the solid diamonds (T_N) and the crosses (T_N from Ref. 2) in Figs. 6(b) and 6(c). Additionally, the boundary that separates the positive (red) and the negative (blue) $\Delta R/R$ signals becomes clear at delay time $t=3$ ps and is evidently within the so-called Nernst region between the doping-dependent lines of T_N and T_c [Fig. 6(c)]. In contrast, the pseudogap temperature T_s (solid squares in Fig. 6) falls as the Pr content decreases, and exhibits totally different dynamics and a totally different doping dependence from those that give rise to the evolution of T_N. Nonetheless, the dominant parts (dark blue area) of Figs. 6(b) and 6(c) with a strong negative signal are confined in between the T_N (solid diamonds) and T_s (solid squares), and move away from T_s toward T_N as the delay time increases. This implies that the relaxation of photoinduced QPs close to T_N occurs much more slowly than that of those close to T_s, which is consistent with the relaxation time of QPs increases slightly within 1–2 ps as decreasing temperatures in Fig. 5. However, the relaxation time of QPs does not monotonously rise in the Nernst region but significantly declines above T_N as shown by the solid lines in Fig. 5. Therefore, it implies that a certain interaction has already existed for paring between carriers above T_c to suppress the relaxation time, which may relate to the glassiness or the so-called noncondensed pairs without the global phase coherence in Chien's scenario.[20,21]

Very recently, Cry-Choinière *et al.*[22] observed two separate Nernst peaks in the stripe ordered Eu-$La_{2-x}Sr_xCuO_4$. One peak near T_c associated with the superconducting fluctuations corresponds to the boundary between T_N and T_c in Figs. 6(b) and 6(c). The other Nernst peak, the so-called QP peak at high temperature associated with the mobile charge carriers, corresponds to the T_s in Figs. 6(b) and 6(c). According to above results, one possible scenario for the time-evolving T-x phase diagram can be organized to figure out how the evolution of the photoinduced QPs from high temperatures to low temperatures. For one specific frame, e.g., $t=1.2$ ps, the photoinduced QPs can be clearly observed in pseudogap region (blue color below T_s) and superconducting region (red color below T_c) simultaneously at the slightly Pr-doping area. Although the photoinduced QPs are only observed between T_s and T_N at deeply Pr doping, after several

picoseconds all of the photoinduced QPs release to the region around T_N [blue color in Fig. 6(c)] and below T_c [red color in Fig. 6(c)] in contrast to the photoinduced QPs with short relaxation time above T_s. Thus, those in the region below T_s and T_c have the same physical origin with different strength for the interaction, e.g., with global phase coherence or not. Furthermore, the mixture between QPs without and with global phase coherence to form the boundary (the area between blue and red color) between T_N and T_c, i.e., the Nernst or superconducting fluctuations region.[20]

IV. SUMMARY

In summary, the change in the transient reflectivity $\Delta R/R$ of $Y_{1-x}Pr_xBa_2Cu_3O_{7-\delta}$ thin films with $x=0$, 0.1, 0.2, and 0.4 was systematically measured using the femtosecond time-resolved spectroscopy. The doping-dependent T_N significantly exceeds T_c, which is related to the Nernst effect, is also clearly observed in the ultrafast responses. Moreover, the correlation among the Nernst effect, the pseudogap, and even the superconducting gap was unambiguously shown in the ultrafast dynamics phase diagram.

ACKNOWLEDGMENTS

We thank the National Science Council of the Republic of China, Taiwan, for financially supporting this research under Contracts No. NSC95-2112-M-009-011-MY3, No. NSC96-2923-M-009-001-MY3, and No. NSC98-2112-M-009-008-MY3, and the Grant MOE ATU Program at NCTU.

[1] Y. Y. Wang, L. Li, and N. P. Ong, Phys. Rev. B **73**, 024510 (2006).
[2] P. C. Li, S. Mandal, R. C. Budhani, and R. L. Greene, Phys. Rev. B **75**, 184509 (2007).
[3] I. Kokanović, J. R. Cooper, and M. Matusiak, Phys. Rev. Lett. **102**, 187002 (2009).
[4] Z. A. Xu, N. P. Ong, Y. Wang, T. Kakeshita, and S. Uchita, Nature (London) **406**, 486 (2000).
[5] D. Podolsky, S. Raghu, and A. Vishwanath, Phys. Rev. Lett. **99**, 117004 (2007).
[6] I. Ussishkin, S. L. Sondhi, and D. A. Huse, Phys. Rev. Lett. **89**, 287001 (2002).
[7] C. W. Luo, P. T. Shih, Y.-J. Chen, M. H. Chen, K. H. Wu, J. Y. Juang, J.-Y. Lin, T. M. Uen, and Y. S. Gou, Phys. Rev. B **72**, 092506 (2005).
[8] S. G. Han, Z. V. Vardeny, K. S. Wong, O. G. Symko, and G. Koren, Phys. Rev. Lett. **65**, 2708 (1990).
[9] J. M. Chwalek, C. Uher, J. F. Whitaker, G. A. Mourou, J. Agostinelli, and M. Lelental, Appl. Phys. Lett. **57**, 1696 (1990).
[10] C. W. Luo, C. C. Hsieh, Y.-J. Chen, P. T. Shih, M. H. Chen, K. H. Wu, J. Y. Juang, J.-Y. Lin, T. M. Uen, and Y. S. Gou, Phys. Rev. B **74**, 184525 (2006).
[11] J. Demsar, B. Podobnik, V. V. Kabanov, Th. Wolf, and D. Mihailovic, Phys. Rev. Lett. **82**, 4918 (1999).
[12] C. W. Luo, M. H. Chen, S. P. Chen, K. H. Wu, J. Y. Juang, J.-Y. Lin, T. M. Uen, and Y. S. Gou, Phys. Rev. B **68**, 220508(R) (2003).
[13] S. J. Liu and Weiyan Guan, Phys. Rev. B **58**, 11716 (1998).
[14] V. V. Kabanov, J. Demsar, B. Podobnik, and D. Mihailovic, Phys. Rev. B **59**, 1497 (1999).
[15] I. P. Hong, J.-Y. Lin, J. M. Chen, S. Chatterjee, S. J. Liu, Y. S. Gou, and H. D. Yang, Europhys. Lett. **58**, 126 (2002).
[16] A. S. Kazeroonian, T. K. Cheng, S. D. Brorson, Q. Li, E. P. Ippen, X. D. Wu, T. Venkatesan, S. Etemad, M. S. Dresselhaus, and G. Dresselhaus, Solid State Commun. **78**, 95 (1991).
[17] K. H. Wu, C. W. Luo, J. Y. Juang, T. M. Uen, and Y. S. Guo, Chin. J. Phys. (Taipei) **38**, 279 (2000).
[18] D. H. Reitze, A. M. Weiner, A. Inam, and S. Etemad, Phys. Rev. B **46**, 14309 (1992).
[19] C. C. Tsuei, C. C. Chi, D. M. Newns, P. C. Pattnaik, and M. Däumling, Phys. Rev. Lett. **69**, 2134 (1992).
[20] C.-C. Chien, Y. He, Q. Chen, and K. Levin, Phys. Rev. B **79**, 214527 (2009).
[21] T. Senthil and P. A. Lee, Phys. Rev. B **79**, 245116 (2009).
[22] O. Cry-Choinière, R. Daou, F. Laliberté, D. LeBoeuf, N. Doiron-Leyraud, J. Chang, J.-Q. Yan, J.-G. Cheng, J.-S. Zhou, J. B. Goodenough, S. Pyon, T. Takayama, H. Takagi, Y. Tanaka, and L. Taillefer, Nature (London) **458**, 743 (2009).